On the onset of the Gulf of Cadiz Coastal Countercurrent

Ana Teles-Machado,[1] Álvaro Peliz,[1] Jesus Dubert,[1] and Ricardo F. Sánchez[2]

Received 20 March 2007; revised 30 April 2007; accepted 10 May 2007; published 16 June 2007.

[1] We investigate the onset of the warm counterflow recurrent in summer periods along the shelf of the Gulf of Cadiz and southwest of Iberia. Fully realistic and idealized numerical configurations are used with the aim of partitioning the different processes at play in the complex circulation of the Gulf of Cadiz. The realistic model simulates in great detail an event of warm counterflow in August 2000. The analysis of the idealized and sensitivity experiments allow us to conclude that the counterflow is mainly wind-driven in response to short but strong Levanter episodes, recurrent after periods of persistent upwelling-favorable situations. **Citation:** Teles-Machado, A., Á. Peliz, J. Dubert, and R. F. Sánchez (2007), On the onset of the Gulf of Cadiz Coastal Countercurrent, *Geophys. Res. Lett.*, *34*, L12601, doi:10.1029/2007GL030091.

1. Introduction

[2] A warm coastal flow developing along the Gulf of Cadiz shelf (Figure 1) is often observed in infrared satellite imagery. This counterflow runs opposite to the typical upwelling coastal circulation, bringing warmer waters from eastern Gulf of Cadiz to the southwest coast of Iberian Peninsula (IP), usually much cooler due to persistent upwelling during summer. Its expression on the SST images has been observed to turn around Cape St Vincente (CSV) and propagate northward along the west coast at times reaching Cape Sines.

[3] A first detailed analysis of this flow structure is presented by *Relvas and Barton* [2002]. The authors analyze a large set of infrared imagery and coastal winds, and report a considerable number of counterflow events. They conclude that the counterflow develops after upwelling relaxation, and conjecture that the mechanism beyond the development of the counterflow is a background alongshore pressure gradient that gets unbalanced during upwelling relaxation and triggers the development of the coastal flow. *Relvas and Barton* [2002] also list a few processes that could generate pressure gradients like: the large scale meridional density gradients, the exchange through the Strait of Gibraltar, and the wind stress-curl near the Iberian margin. The change in coastline orientation, near CSV is certainly responsible for causing wind field heterogeneities and localized curls. *Sanchez et al.* [2006] support that the onset of an alongshore pressure gradient in the south coast is better correlated with west coast alongshore coastal winds than with Gulf of Cadiz winds.

[4] An additional process that may be of importance in the Gulf of Cadiz system is described by *Gan and Allen* [2002] for the Oregon coast. Strong upwelling jets may generate local alongshore pressure gradients in the lee of capes and promontories that drive innershelf counterflows during upwelling relaxation.

[5] *Garcia-Lafuente et al.* [2006] describe a set of ADCP observations along the Gulf of Cadiz and note that the warm counterflow may develop simultaneously with intense equatorward upwelling currents along the slope. The authors demonstrate that the counterflow is independent of pressure gradients external to the coast since the flows may be both active. *Garcia-Lafuente et al.* [2006] speculate that an important contribution to the warm counterflow may be associated with the warming of the coastal waters produced by tidally driven flooding of very shallow inland areas (bays and estuaries) abundant along the Gulf of Cadiz coast.

[6] With the objective of bringing insight into the onset of the counterflow we conducted a realistic numerical modeling study based on the numerical configurations of A. Peliz et al. (Surface circulation in the Gulf of Cadiz: 1. Model and mean flow structure, submitted to *Journal of Geophysical Research*, hereinafter referred to as Peliz et al., submitted manuscript, 2007). The experiment concentrates on the counterflow event of August 2000 [*Sanchez et al.*, 2006] and both realistic and idealized runs are described.

2. Model Configuration

[7] The simulations described below were performed using the Regional Ocean Modeling System (ROMS) with nesting capabilities [*Shchepetkin and McWilliams*, 2005; *Penven et al.*, 2006]. Two domains were defined (depicted in Figure 1) with a grid spacing of approximately 10 km and 3.5 km, respectively the medium domain (MD) and smaller domain (SD). MD was initialized with data from a previous experiment with a larger grid, encompassing all the mid latitude eastern north Atlantic (spin-up from Levitus climatology during 4 years [*Levitus and Boyer*, 1994; *Levitus et al.*, 1994]). Mediterranean Water (MW) is explicitly resolved through the imposition of an inflow/outflow condition at the Strait of Gibraltar; boundary and initial conditions were obtained from an initial model run of a large scale domain. A detailed description of the model configuration is presented by Peliz et al. (submitted manuscript, 2007).

[8] WRF atmospheric model (http://www.wrf-model.org/) was used to create atmospheric forcing fields at 15 km resolution. WRF winds together with QuickScat and NCEP-2 wind data, were compared to winds obtained by an ocean buoy located inside Gulf of Cadiz (see point A, Figure 1). The WRF simulated winds have proven to be the ones which best represent intensity and direction (Figure 2).

3. Numerical Experiments

[9] Table 1 displays the different experiments that were conducted. The first experiment (1-BC) is the most realistic

[1]Centro de Estudos do Ambiente e do Mar (CESAM), Departamento de Física, Universidade de Aveiro, Aveiro, Portugal.
[2]Instituto Español de Oceanografía (IEP), Santander, Spain.

0094-8276/07/2007GL030091$05.00

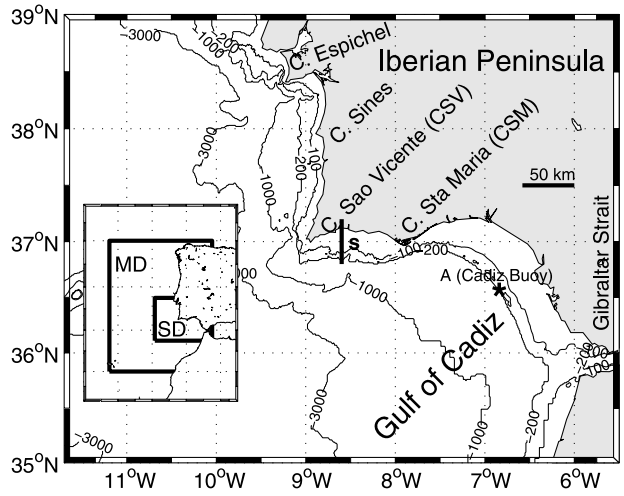

Figure 1. General bathymetry and coastal morphology of IP region, with important locations referred in the text. The represented area corresponds to the small model domain (SD). Inset shows IP region and model domains, medium (MD) and small (SD).

case, where the external large-scale forcing, Mediterranean water and WRF forcing are used. The dependence of the response on the large scale circulation is investigated in a second experiment (2-Hom) where initial fields and climatology are horizontally homogenous, using temperature and salinity profiles typical of the region, extracted from Levitus Climatology. This way, initial spatial horizontal variability of temperature and salinity was ignored, eliminating baroclinic pressure gradients, and permanent pressure gradients due to large scale circulation. The effect of the Mediterranean Undercurrent (3-nMW) is examined by shutting off the Strait of Gibraltar exchange condition (a closed eastern boundary was used in this case). To test hypothesis regarding wind stress forcing, three experiments were conducted by varying wind fields: (4-NS) setting zonal component to zero (north-south only); (5-EW) setting meridional component to zero (east-west only); (6-W) setting meridional component to zero and allowing only westerlies. These experiments were performed with initial homogeneous fields and without Strait of Gibraltar exchange condition, to simplify the configurations and to isolate the direct effect of the wind. All other model characteristics (grids and parameters) are the same as for the basic case experiment, except that the boundary conditions are also homogeneous in MD and the model starts from resting state.

Table 1. Summary of the Numerical Experiments Denoted by a Description of the Differences From the Basic Case and the Abbreviations Used to Identify the Experiments in the Figures

Description	Abbreviation
Basic case[a]	BC
Homogeneous initial horizontal fields[b]	Hom
Without Mediterranean Water[a]	nMW
Wind - north-south only[b]	NS
Wind - east-west only[b]	EW
Wind - westerlies only[b]	W

[a]Initial fields and climatology from larger scale spinup.
[b]Initial fields and climatology from Levitus homogenized fields.

4. The Counterflow Event in August 2000

[10] Figures 3a and 3b represent SST fields for 4 and 12 August, obtained from satellite data. The cold waters along the west coast (visible in Figure 3a of 4 August) indicate a situation of developed upwelling that preceded the countercurrent event. In the south coast, a filament grew to the east, inside Gulf of Cadiz, that is bringing cold waters from the west to the south coast, in association with the Gulf of Cadiz slope Current (GCC) as described by Peliz et al. (submitted manuscript, 2007). It is clear the presence of an intrusion of warm waters propagating westward along the south coast, the Gulf of Cadiz Coastal Countercurrent (G3C). The two situations displayed in the same figure represent different stages of the G3C event (4 August an early stage and 12 August an advanced stage). By 12 August, G3C has turned around CSV and propagated northward along Iberian west coast. The cold water filament is still visible by 12 August in satellite imagery, but it has been displaced offshore.

[11] The entire episode lasts nearly 16 days, from 27 July to 12 August, which is nearly coincident with an episode of easterlies in the south coast. In Figure 2, u (west/east) and v (south/north) components of the wind are represented for

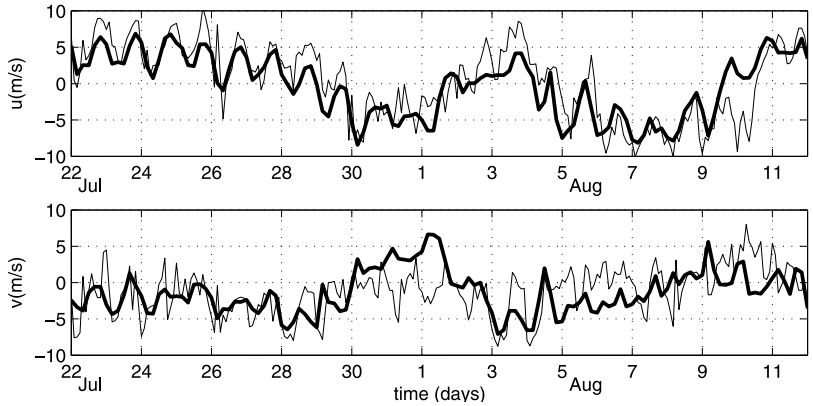

Figure 2. Wind components inside Gulf of Cadiz (6.93 °W, 36.5°N-point A in Figure 1): (top) zonal component (west-east) and (bottom) meridional component (north-south). In both plots, WRF model output is shown in bold and buoy observation as a thinner line [retrieved from Spanish Institution, Puertos del Estado-Redes de Medida].

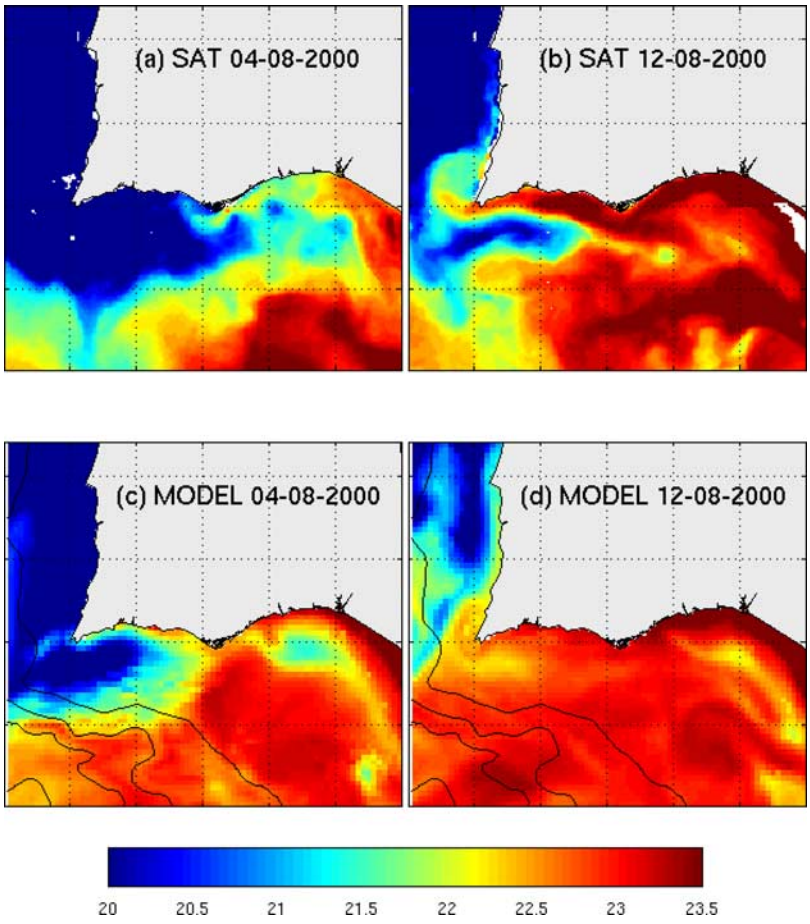

Figure 3. Sea surface temperature for (a) 4 August and (b) 12 August, obtained from satellite data (NOAA/AVHRR), and for (c) 4 August and (d) 12 August, from model results.

a point located inside Gulf of Cadiz (see point A, Figure 1). If u is positive/negative, wind is upwelling/downwelling favorable in the south coast. The countercurrent episode happens under the presence of downwelling winds.

5. Basic Case

[12] Figures 3c and 3d show outputs of the BC experiment for the same days represented in satellite images. The model results include some of the features usually observed in typical SST imagery of Gulf of Cadiz, namely: the cold band of upwelled waters of the west coast (weaker in the model); the intrusion of west coast upwelled waters along the southern coast slope (cold filament, also weaker in the model results); the significant warming in the Gulf of Cadiz shelf zone; and the warm counterflow (G3C) described below, that is reproduced in the same days observed in satellite imagery and with similar across shore length scales.

[13] By 27 July (not shown), a counterflow is first noticeable in the south coast, close to the shore and to the east of important capes (CSV and CSM), although the winds only revert to downwelling favorable (negative u) by 29 July (Figure 2, top plot). At an advanced stage (see Figure 4a for both temperature and currents at 10 m depth by 8 August), it extends along all the southwest coast, from Strait of Gibraltar to Cape Espichel. Although the thermal expression of the counterflow is visible only till Cape Sines, the countercurrent is present over all the domain. In the eastern Gulf of Cadiz, where the shelf is broader, its lateral width is about 20 km, while along the south and west coasts of Portugal it narrows to about 10 km. Current velocities in the south coast are around 0.2 m s^{-1} and after turning around CSV, the countercurrent gets more intense, reaching 0.4 m s^{-1} near CSV and Cape Sines. This value is coincident with that observed near CSV in a cruise in June 1994, during an episode of the countercurrent [*Relvas and Barton*, 2005]. Westward transport within the countercurrent, calculated for section S (Figure 1), reaches a maximum of 0.13 Sv by 7 August.

[14] By 12 August (see Figure 3), G3C has turned around CSV and propagated northward along the Iberian west coast; in fact, by this day the current has already inverted to southward again (not shown), but this is not visible in SST field. The model results indicate that the SST signal may lag the current reversal.

6. Other Experiments

[15] Figure 4 represents horizontal distribution of temperature and horizontal velocity at 10 m depth, by 8 August, for the different experiments listed in Table 1. This date was chosen because by this day the countercurrent is visible in the entire domain.

[16] The importance of the large scale circulation is examined in experiment 2-Hom (Table 1). The horizontal fields, (10 m depth) of temperature and velocity for this

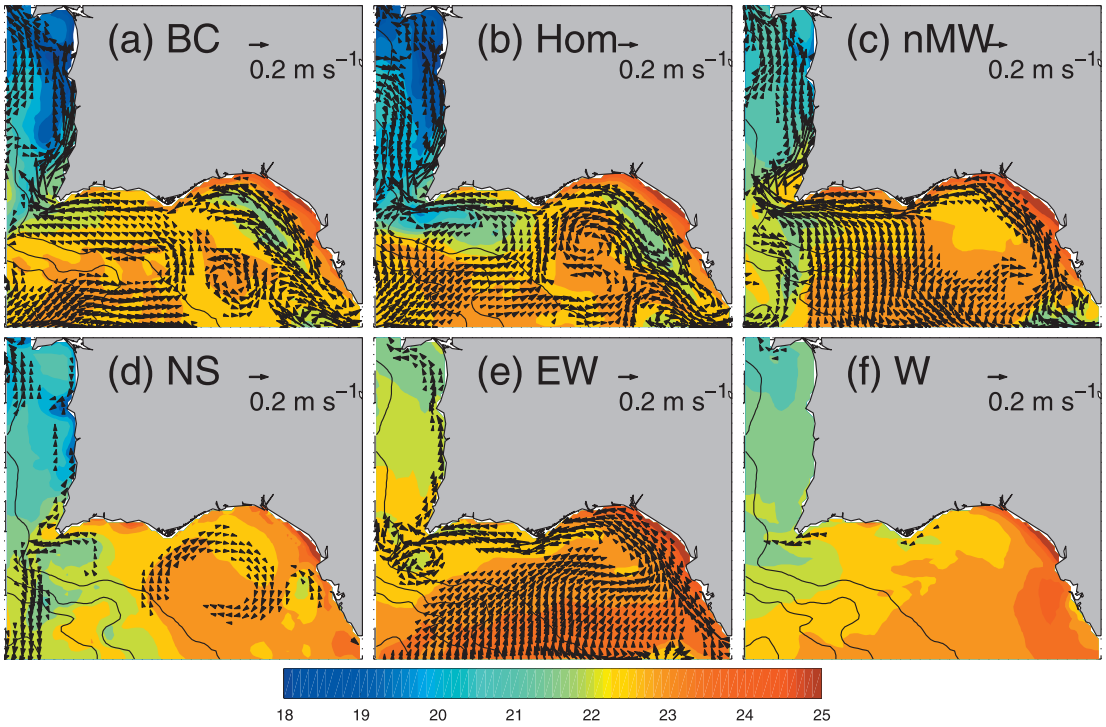

Figure 4. The 10 m depth horizontal fields of temperature and velocity for 8 August: (a) BC, (b) nMW, (c) Hom, (d) NS, (e) EW and (f) W. (Vectors with absolute values below 0.05 m s^{-1} were not plotted.)

experiment are presented in Figure 4b. The behavior is very similar to the BC experiment (Figure 4a), in what concerns the generation and propagation of the countercurrent. It is possible to conclude that the large scale meridional gradients do not play an important role in the onset and propagation of the countercurrent.

[17] The importance of Mediterranean Water is examined by comparing Figure 4c horizontal fields, from experiment 3-nMW (Table 1), with the basic case (Figure 4a). The experiment without MW does not reach in the west coast the developed upwelling stage observed in BC experiment. The intrusion of west coast cold upwelled waters to the south coast is not reproduced. In spite of the differences in circulation and temperature fields, the countercurrent is reproduced, and its onset occurs in a similar way, being first identified to the east of CSV and CSM in the south coast. Model results show an advanced stage of the G3C, that extends from Strait of Gibraltar to Cape Espichel, just as in the BC experiment (Figure 4a). Despite of being essential to reproduce the circulation inside Gulf of Cadiz, the Strait of Gibraltar exchange condition does not influence directly the onset of the countercurrent.

[18] In experiment 4-(NS) (Table 1), the zonal component (u) of the wind was set to zero, meaning that wind is only able to reproduce upwelling in the west coast. The purpose of this experiment is to investigate the importance of west coast northerlies relaxation on the onset of the countercurrent. The results are presented in Figure 4d. The countercurrent is not reproduced along the entire south coast, as happened in previous experiments; but only in the vicinity of CSV. A counterflow develops also in the west coast, probably associated with relaxation of west coast upwelling winds that relaxed just by this day, turning into southerly (not shown).

[19] In experiment 5-(EW), it was checked the importance of the local (south coast) alongshore winds to the onset and behavior of the countercurrent (Figure 4e). Upwelling is absent on the west coast, as was expected, because west coast upwelling winds were set to zero. The countercurrent is present over all the domain, from Strait of Gibraltar till the northern boundary (Cape Espichel), although it is weaker along west coast than in BC experiment. Its onset happens to the east of south coast capes, as in BC experiment.

[20] Experiment 6-(W) is similar to the previous one, but easterly winds were set to zero, to study the importance of the downwelling winds to the countercurrent. Results are presented in Figure 4f. Although the coastal flow is in the right direction, the countercurrent is hardly reproduced (note that velocities <0.05 m s^{-1} are not represented).

7. Discussion and Conclusion

[21] An event of coastal counterflow along the Gulf of Cadiz coast was observed in the summer of 2000. Simulations using ROMS with nested domains centered in the Gulf of Cadiz, forced by high resolution WRF outputs, were conducted, with the aim of reproducing the major features of the observed event and isolating the different processes at play in its formation. The model results reproduce well the progression of the countercurrent, showing good agreement with SST fields from satellite imagery.

[22] Results from BC experiment show that the warm countercurrent is first noticeable in the south coast, to the east of important capes (CSV and CSM), revealing that the coastline irregularities might be important to the onset of the counterflow.

[23] The countercurrent was reproduced in experiment 2-(Hom) where initial fields were set to homogeneous, so it does not seem to depend on any extra-coastal (large scale) permanent pressure gradient. Direct influence of the MW in the onset of the counterflow was excluded in experiment 3-(nMW). In fact, the countercurrent was reproduced in all the experiments, except in those where zonal winds were suppressed. Experiment 4-(NS), where the u-wind component (alongshore component in the south coast) was set to zero, does not reproduce the countercurrent. This indicates that the development of G3C is not related with west coast winds, but with local Gulf of Cadiz winds. In experiment 6-(W) the north-south component is set to zero and only westerlies are allowed (upwelling favorable along the south coast). After wind relaxation a weak counterflow is reproduced, in a similar mechanism to that proposed by *Gan and Allen* [2002], as it happens in the times of relaxation and to the east of south coast capes. However, easterly winds (downwelling favorable) are essential to generate an intense and realistic counterflow.

[24] A considerable number of counterflow episodes reported by *Relvas and Barton* [2002] and illustrated with SST images are associated with a change in the atmospheric situation from north to east winds (Levanter). This fact could be checked from the time series of weather types (WT) of *Trigo and DaCamara* [2000]. The events: 1/Sep/1982; 20/Jul/1986; 19/Sep/1988; 1/Oct/1988; 10/Aug/1991; 4/Aug/1992 and our case 4/Aug/2000, all correspond to a change in WT from NE to E.

[25] In conclusion, the onset of a very weak innershelf counterflow may happen right after upwelling relaxation, and the current is first noticeable east of south coast capes (CSV and CSM). However, a full developed counterflow is only observed after the onset of the Levanter winds, typical of many post upwelling episodes. Our results indicate that the G3C is a wind-driven downwelling jet. However, a deeper analysis of the dynamics of the countercurrent (momentum balance like, e.g., *He et al.* [2004]) should be addressed in a future study. In many cases, the SST signature of the counterflow on the west coast is still visible while the winds changed back to upwelling-favorable. Our model results show that the warm signature may lag the current inversion to southward again, indicating that an analysis of the SST fields alone may be misleading.

[26] **Acknowledgments.** This work was funded by the Fundação para a Ciência e a Tecnologia (FCT) through the research contracts ProFit (PDCTE/CTA/50386/2003), LobAssess (POCTI/BIA-BDE/59426/2004) and Clibeco (POCI/CLI/57752/2004). A. Teles-Machado has been the recipient of a grant from the Centre for Environmental and Marine Studies (CESAM), financed by FCT. QuickSCAT data were provided by IFREMER at the Department of Oceanography from Space (LOS + CERSAT). NCEP/DOE 2 Reanalysis data were provided by the NOAA/OAR/ESRL PSD, Boulder, Colorado, USA, from their Web site at http://www.cdc.noaa.gov/.

References

Gan, J., and J. S. Allen (2002), A modeling study of shelf circulation off northern California in the region of the Coastal Ocean Dynamics Experiment: Response to relaxation of upwelling winds, *J. Geophys. Res.*, *107*(C9), 3123, doi:10.1029/2000JC000768.

Garcia-Lafuente, J., et al. (2006), Water mass circulation on the continental shelf of the gulf of cadiz, *Deep Sea Res., Part II*, *53*, 1182–1197.

He, R., Y. Liu, and R. H. Weisberg (2004), Coastal ocean wind fields gauged against the performance of an ocean circulation model, *Geophys. Res. Lett.*, *31*, L14303, doi:10.1029/2003GL019261.

Levitus, S., and T. Boyer (1994), *World Ocean Atlas 1994*, vol. 4, *Temperature*, *NOAA Atlas NESDIS 4*, NOAA, Silver Spring, Md.

Levitus, S., R. Burgett, and T. Boyer (1994), *World Ocean Atlas 1994*, vol. 3, *Salinity*, *NOAA Atlas NESDIS 3*, NOAA, Silver Spring, Md.

Penven, P., L. Debreu, P. Marchesiello, and J. C. McWilliams (2006), Evaluation and application of the ROMS 1-way embedding procedure to the central California upwelling system, *Ocean Modell.*, *12*, 157–187.

Relvas, P., and E. D. Barton (2002), Mesoscale patterns in the Cape São Vicente (Iberian Peninsula) upwelling region, *J. Geophys. Res.*, *107*(C10), 3164, doi:10.1029/2000JC000456.

Relvas, P., and E. Barton (2005), A separated jet and coastal counterflow during upwelling relaxation off Cape São Vicente (Iberian Peninsula), *Cont. Shelf Res.*, *25*, 29–49.

Sanchez, R., E. Mason, P. Relvas, A. J. da Silva, and A. Peliz (2006), On the inshore circulation in the northern Gulf of Cadiz, southern Portuguese shelf, *Deep Sea Res., Part II*, *53*, 1198–1218.

Shchepetkin, A. F., and J. C. McWilliams (2005), The regional oceanic modeling system (ROMS): A split-explicit, free-surface, topography-following-coordinate oceanic model, *Ocean Modell.*, *9*(4), 347–404.

Trigo, R., and C. DaCamara (2000), Circulation weather types and their impact on the precipitation regime in Portugal, *Int. J. Climatol.*, *20*, 1559–1581.

J. Dubert, Á. Peliz, and A. Teles-Machado, CESAM, Departamento de Física, Universidade de Aveiro, Aveiro P-3800-193, Portugal. (atmachado@fis.ua.pt)

R. F. Sánchez, IEO, Promontorio de S. Martín s/n P.O. Box 240 E-39080, Santander, Spain.